GEOPHYSICAL RESEARCH LETTERS, VOL. 27, NO. 22, PAGES 3747-3750, NOVEMBER 15, 2000

Propagation of North Pacific interdecadal subsurface temperature anomalies in an ocean GCM

Masami Nonaka[1] and Shang-Ping Xie

International Pacific Research Center/SOEST, University of Hawaii, Honolulu, Hawaii

Abstract. Propagation of subsurface North Pacific interdecadal variations is investigated with an ocean general circulation model forced by observed sea surface temperature anomalies. Subsurface temperature anomalies subducted in the central subtropical North Pacific take a more westward pathway than a passive "temperature" tracer and reach the western boundary to the north of the bifurcation latitude. This prevents them from extending into the equator. On the boundary between the subtropical and the subarctic gyres, on the other hand, the upper 500 m heat content anomaly is found to propagate eastward as high vertical modes of Rossby waves advected by the mean eastward current. This notion is supported by a sign reversal in temperature anomaly underneath.

1. Introduction

Decadal/interdecadal variations in the North Pacific Ocean and the global atmosphere have been described in many studies [*Tanimoto et al.,* 1993; *Deser et al.,* 1996, and references therein]. Equatorward propagation of subtropical sea surface temperature (SST) anomalies through the subsurface pathway provides the delay for the slow variations in the *Gu and Philander* [1997] mechanism, whereas clockwise propagation of upper ocean heat content within the subtropics is a key process in *Latif and Barnett* [1994]. In both hypotheses, how temperature anomalies propagate is crucially important.

For the former hypothesis, analysis of historical data confirms a southwestward propagation of subsurface interdecadal temperature anomalies from the central North Pacific to the tropics [*e.g., Deser et al.,* 1996], but *Schneider et al.* [1999] can trace these southwestward propagating anomalies only to 18°N and suggested that their final extension from the subtropics into the equator is mainly forced by local wind-stress variations. On the other hand, ocean general circulation model (OGCM) results suggest the North Pacific decadal SST anomalies exist within the exchange window, from which subducted water goes to the equatorial region [*Nonaka et al.*, 2000].

Then, what prevents the subtropical SST anomalies from entering the equator, given that part of them are located within the exchange window (Fig. 1)? Noting that interdecadal SST anomalies in the exchange window change sign, *Nonaka et al.* [2000] suggest that isopycnal mixing dampens subsurface temperature anomalies. Whereas Nonaka et al. treated temperature anomaly as a passive tracer, temperature is a dynamically active variable that interacts with the density and flow fields unless compensated by salinity anomalies. Using simple ventilated thermocline model, *Huang and Pedlosky* [1999] found that the ocean response to surface density anomalies takes the form of higher baroclinic modes of Rossby waves, and *Liu and Shin* [1999] pointed out that it has propagation characteristics that differ from mean current advection.

The present study extends Liu and Shin's and Nonaka et al.'s work by forcing an OGCM with observed interdecadal SST anomaly pattern and allowing temperature anomalies to interact with the flow field. We will compare the temperature anomalies in the passive and active runs, particularly their vertical structure and isopycnal distribution. We are interested in whether and how the differences in propagation characteristics between the passive and active tracers affect the entrance of temperature anomalies into the equator.

In addition to the equatorward propagation of temperature anomalies, we are also interested in an eastward-propagating upper ocean heat content anomaly (HCA) in the northern subtropics on decadal/interdecadal time scales that is reported by *Latif and Barnett* [1994] and *Zhang and Levitus* [1997] in a coupled GCM and observations, respectively. This eastward propagation of HCA is puzzling given that sea level height variability at this latitude generally shows a westward phase propagation [*e.g., Chelton and Schlax,* 1996].

In the rest of this paper, section 2 describes the model and the experiment procedures. Section 3 focuses on the equatorial propagation of anomalies subducted in the subtropics. Section 4 investigates the model response farther to the north to see if there is an eastward propagation of HCA as suggested by previous studies.

2. Model

We use the GFDL MOM 1.1 [*Pacanowski et al.*, 1991]. The model covers the portion of the Pacific from 50°S to 60°N and has realistic coastline and bottom topography, with the maximum depth at 5000 m. The horizontal and vertical eddy viscosities are constant at 5.0×10^7 and 10.0 $cm^2 s^{-1}$, respectively. Temperature and salinity are mixed both along isopycnal surfaces and diapycnally with diffusivities of 2.0×10^7 and 0.3 $cm^2 s^{-1}$, respectively. At the sea surface, the monthly climatological wind stress is applied, and temperature and salinity are restored to the monthly climatological values (control run) with restoring time of 14 days for the upper 10-m water column. The horizontal resolution is 1 degree, and there are 41 levels in the vertical.

[1]Also Frontier Research System for Global Change, Tokyo, Japan

Paper number 2000GL011488.
0094-8276/00/2000GL011488$05.00

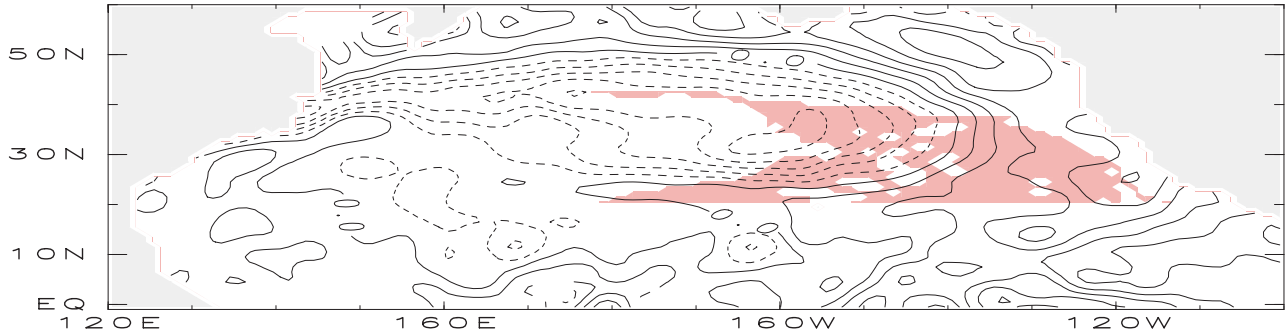

Figure 1. Winter (Jan.-Mar.) SST difference between 1977–87 and 1965–75, calculated based on Comprehensive Ocean Atmosphere Data Set. Contour intervals are 0.2°C with negative values dashed. The subtropical–tropical exchange window in the model is shaded.

The model is integrated for 30 years and reaches a nearly steady state (for details, see *Nonaka and Takeuchi* [2000]).

Observed interdecadal SST anomalies (Fig. 1) north of 20°N are added to the climatology to construct a new reference field, toward which the model SST is restored (the SSTA run). The SSTA and control runs are further integrated for 19 years from the year 30 field of the control and the difference of two runs will be analyzed.

In the third model integration, the same SST anomalies are injected into the model ocean and advected by the model flow field as a passive tracer (passive tracer run; *Nonaka et al.* [2000]). We will compare temperature anomalies in the SSTA run and this passive tracer.

3. Equatorward propagation

Maximum subsurface temperature anomalies are found around the σ_θ=25.5 isopycnal surface in the model central North Pacific. Fig. 2a shows the temperature anomalies in year 19 on this isopycnal surface, which extend southwestward and create a tongue-like structure that reaches the western boundary. This distribution of the temperature anomalies is consistent with observations, but their amplitudes are weaker [*Zhang and Levitus* 1997; *Schneider et al.* 1999]. The negative temperature anomalies originate from the oval-shaped pattern of SST anomalies in the central North Pacific (Fig. 1) and spread almost in the direction of the ocean circulation. This is best seen in Fig. 2b for the passive tracer run where the ocean currents are visualized by the trajectories. Almost all the trajectories that carry negative tracer into the equator go through the western boundary. Eastern positive anomalies also subduct and propagate southwestward, but dissipate due to mixing with the western negative anomalies during their equatorward propagation [*Nonaka et al.* 2000].

Although temperature anomalies within the subtropical gyre look similar between the SSTA and passive tracer

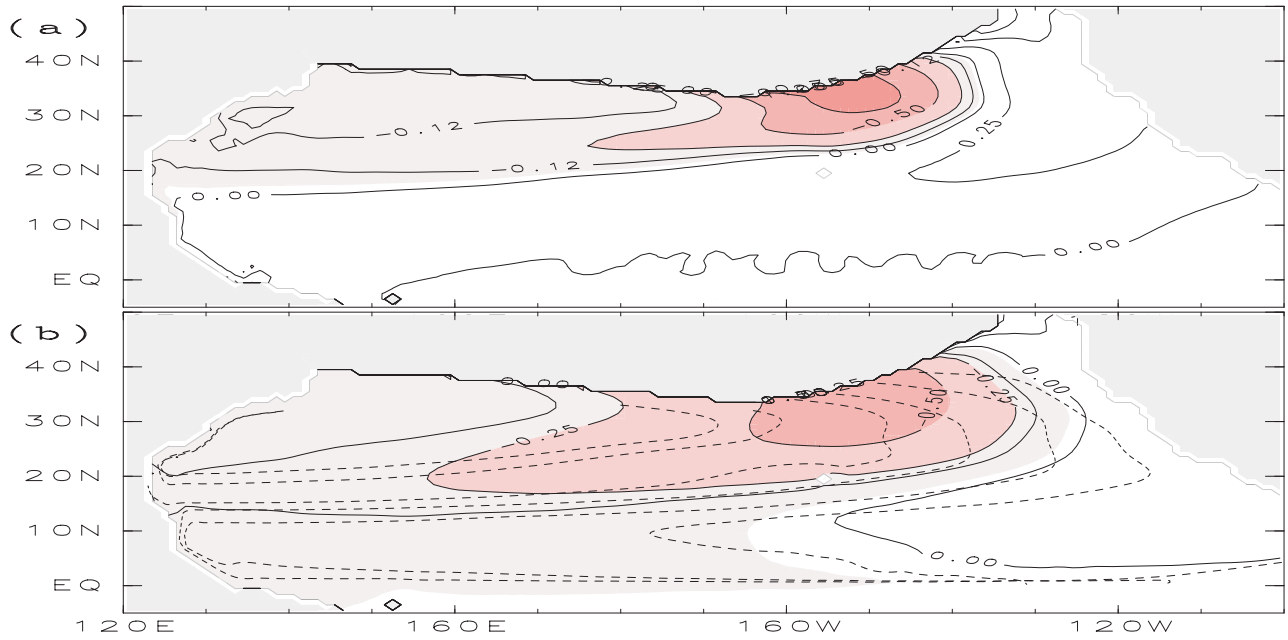

Figure 2. (a) Temperature difference between the SSTA and control runs on the σ_θ=25.5 surface of the control run (shade < -0.05°C). (b) Passive tracer concentration (solid lines) on the σ_θ=25.5 surface along with water parcel trajectories (dashed lines). Trajectories are based on annual mean velocity field. Contour intervals are 0.25°C, with contours of -0.12 and -0.17 added for (a) and (b), respectively.

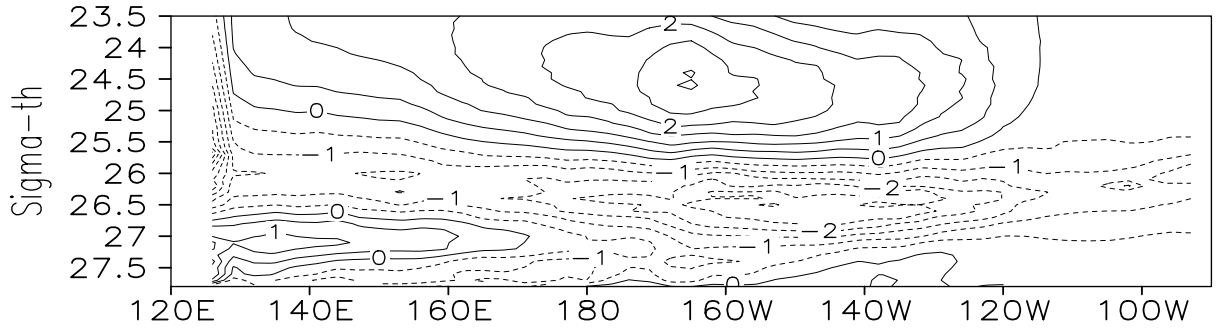

Figure 3. Longitude-density section of isopycnal depth difference at 15°N near the bifurcation latitude for the western boundary currents. Contour intervals are 0.5 m with negative value dashed.

runs, important differences exist with regard to their further southward extension into the equator. The temperature anomalies in the SSTA run extend in a slightly more zonal direction than in the passive tracer run (Fig. 2a, b), consistent with *Liu and Shin's* [1999] idealized experiment. THe background potential vorticity (PV) field in our model is different. Whereas PV decreases monotonically westward in Liu and Shin's with zonally uniform forcing, southwestward-propagating anomalies are found around a zonal PV minimum in this GCM [*Xie et al.* 2000]. Liu and Shin suggest that subducted temperature anomalies, as an active tracer, induce high baroclinic modal structure in the vertical, and therefore propagate along characteristics slightly different from mean flow trajectories.

Indeed, our model longitude-density section at 15°N (Fig. 3) shows layered structures with sign alternating in the vertical, indicative of the second or third baroclinic mode.

The passive tracer field on the σ_θ=25.5 surface (Fig. 2b) showed that the center of the negative tracer tongue arrives at the western boundary at 15°N near the bifurcation latitude of the western boundary currents (see the trajectories in Fig. 2b). As a result, the southern part of the negative tracer tongue can extend to the equatorial region. In the active tracer run, by contrast, the center of the negative anomaly tongue hits the western boundary at a much higher latitude north of the bifurcation latitude. This change in anomaly propagation characteristics has important consequences to its equatorward extension and appears to explain the Schneider et al. results that observed interdecadal temperature anomalies do not find their way into the equator but somehow get lost at 18°N.

Unlike the passive tracer, the active tracer can still propagate equatorward from the north of the bifurcation latitude as a coastal Kelvin wave. It decays rapidly on the way to the equator, however, both because the northward western boundary current slows its phase speed and because of its small vertical and horizontal scales. The strong coastal trapping of negative anomalies south of 15°N can be seen in Fig. 2a as compared to the passive tracer runs where they have broader zonal scales (Fig. 2b).

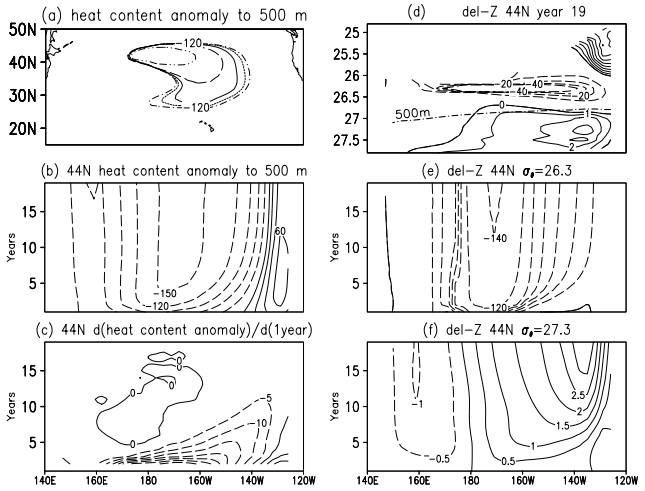

Figure 4. (a) Time evolution of the HCA=-120°C·m contour from year 2 (two dot dash) to year 10 (dot dash) at a two-year interval. (b) Longitude-time sections of HCA and (c) HCA time derivative at 44°N. Contour intervals are 30 in (b) and 5°C·m in (c). (d, e, f) Isopycnal depth anomalies along 44°N: (d) Longitude-density section at year 19, with contour intervals of 1 (10) m for positive (negative), dot-dashed line shows 500 m depth; Longitude-time sections on (e) σ_θ=26.3 and (f) 27.3. Contour intervals are 20 m for (e) and 0.5 m for (f). In all figures other than (a), negative values are dashed.

4. Eastward propagation of HCA in the northern subtropics

Fig. 4a shows the time evolution of the upper 500 m HCA exceeding -120°C·m from year 2 to year 10 in the SSTA run. The strong negative HCA displays an apparent eastward propagation in the subtropics north of 35°N, which can be better seen in longitude-time sections of HCA and its time derivative along 44°N (Figs. 4b and c). These HCAs are not caused by recirculating temperature anomalies subducted in the subtropics, but are forced locally as they appear as soon as SSTAs are imposed. It is worth noting that their eastward propagation takes place under the forcing of stationary SSTAs.

Fig. 4d shows the longitude-density section of isopycnal depth anomalies along 44°N in year 19. In the central and eastern North Pacific, the depth anomalies change sign in the vertical with the node around 500 m, a structure indicative of the second vertical mode. In the western Pacific, on the other hand, they show a vertical structure of the first mode, with the negative sign throughout the depth. Figs. 4e and 4f show the temporal development of these baroclinic structures. On the σ_θ=27.3 surface which does not outcrop in the North Pacific, the depth anomalies are induced by the formation of baroclinic modes in response to the surface forcing. An eastward development of positive anomalies can be clearly seen east of 180° in association with emergence of

negative anomalies above at the σ_θ=26.3 surface. West of 180°, on the other hand, negative anomalies appear on the deeper isopycnal surface as part of the first baroclinic modal structure.

Thus, the interdecadal SST anomalies force the first and second vertical modes of Rossby waves. The first mode propagates westward while the second mode, with a slower intrinsic phase speed, is advected by the eastward mean flow and thus shows an apparent eastward propagation.

5. Summary and Discussion

We forced a realistic OGCM with observed interdecadal SST anomalies and identified two major propagation signals. Within the subtropical gyre, temperature anomalies subducted in the central North Pacific propagate southwestward as high vertical modes of Rossby waves, while at higher latitudes, SST anomalies force a second baroclinic mode of Rossby waves that propagate eastward. The former signal is observed in the North Pacific [*Deser et al*, 1996] and at the heart of the Gu-Philander mechanism. Almost all temperature anomalies subducted in the central North Pacific arrive at the western boundary north of the bifurcation latitude, and little anomalies are found to enter the equator. This is in contrast to a passive tracer experiment where some anomalies find their ways into the equator mainly through the western boundary region, as the trajectories suggest. We show that this difference in the equatorward propagation of anomalies is due to that in propagation characteristics in the subtropical gyre; high baroclinic modes of Rossby waves propagate in a more zonal direction than a passive tracer. This demonstrates that passive trajectories are not a reliable diagnosis for propagation of temperature anomalies.

Thus, the equatorward propagation of temperature anomalies subducted in the subtropical North Pacific is a delicate matter, strongly dependent on the location of SST anomalies relative to the exchange window. In reality, the atmospheric stationary waves play an important role in determining the geographic location of mid-latitude SST anomalies. But, the simulation of these stationary waves are highly model-dependent and can be substantially different from observations. The efficiency for subducted anomalies to arrive at the equator may therefore vary from one coupled GCM to another. As a result, mechanisms for decadal variability may also vary among the coupled models.

Eastward propagating HCAs, a key process of the Latif-Barnett mechanism, are found in our model under the stationary SST forcing. These eastward-propagating HCAs in the northern subtropics are associated with the second baroclinic mode of Rossby waves advected by mean eastward currents. This reconciles the Latif-Barnett hypothesis with satellite observations that SSH anomalies tend to propagate westward, because the first baroclinic mode has a much stronger signature in SSH than higher vertical modes. Most analyses of decadal/interdecadal North Pacific variability use hydrographic data above 500 m, which are not adequate to separate the first from higher vertical modes, as our model indicates that the second mode has its nodal point at 500 m (Fig. 4d). Downward extension of historical datasets/future observation is thus crucial given that the first and higher baroclinic modes propagate in opposite directions on strong eastward currents.

Here we used the climatological wind stress field and focused on temperature anomalies forced by SST anomalies. Wind stress variations are also important for subsurface variability. Wind stress variations tend to preferably force the first baroclinic Rossby waves [*e.g., Liu and Zhang,* 1999] that propagate westward. Their reflection on the western boundary into the coastal Kelvin waves provides yet another mechanism for the subtropics to affect the equatorial region [*Lysne et al.*, 1997]. The relative importance between this wind-forced first vertical mode and SST-forced higher modes needs to be assessed.

Acknowledgments. We thank Drs. K. Takeuchi, Z. Liu and J. McCreary for helpful discussions. This study is supported by the Frontier Research System for Global Change. The figures were produced by GFD-DENNOU library and GrADS. SOEST contribution number 5267. IPRC contribution number 59.

References

Chelton, D. B., and M. G. Schlax, Global Observations of Oceanic Rossby Waves, Science, *272,* 234-238, 1996.

Deser, C., M. A. Alexander, and M. S. Timlin, Upper-Ocean Thermal Variations in the North Pacific during 1970–1991, J. Climate, *9,* 1840–1855, 1996.

Gu, D. and S. G. H. Philander, Interdecadal Climate Fluctuations That Depend on Exchanges Between the Tropics and Extratropics, Science, *275,* 805-807, 1997.

Huang, R. X. and J. Pedlosky, Climate Variability Inferred from a Layered Model of the Ventilated Thermocline, J. Phys. Oceanogr., *29,* 779-790, 1999.

Latif, M. and T. P. Barnett, Causes of Decadal Climate Valiability over the North Pacific and North America, Science, *266,* 634-637, 1994.

Liu, Z., and S.-I. Shin, On thermocline ventilation of active and passive tracers, Geophys. Res. Lett., *26,* 357-360, 1999.

Liu, Z., and R. H. Zhang, Propagation and Mechanism of Decadal Upper-Ocean Variability in the North Pacific , Geophys. Res. Lett., *26,* 739-742, 1999.

Lysne, J., P. Chang, and B. Giese, Impact of the extratropical Pacific on equatorial variability, Geophys. Res. Lett., *24,* 2589-2592, 1997.

Nonaka, M., S.-P. Xie, and K. Takeuchi, Equatorward spreading of a passive tracer with application to North Pacific interdecadal temperature variations, J. Oceanogr., *56,* 173-183, 2000.

Nonaka, M., and K. Takeuchi, Tropical subsurface salinity and tritium distributions in a Pacific GCM: Their differences and formation mechanisms, J. Phys. Oceanogr., revised, 2000.

Pacanowski, R. C., K. W. Dixon and A. Rosati, The GFDL Modular Ocean Model Users Guide, *GFDL Ocean Group Tech. Rep. No. 2,* 1991.

Schneider, N., A. J. Miller, M. A. Alexander, and C. Deser, Subduction of Decadal North Pacific Temperature Anomalies: Observations and Dynamics, J. Phys. Oceanogr., *29,* 1056-1070, 1999.

Tanimoto, Y., N. Iwasaka, K. Hanawa and Y. Toba, Characteristic Variations of Sea Surface Temperature with Multiple Time Scales in the North Pacific, J. Climate, *6,* 1153-1160, 1993.

Xie, S.-P., T. Kunitani, A. Kubokawa, M. Nonaka, and S. Hosoda, Interdecadal thermocline variability in the North Pacific for 1958-1997: A GCM simulation, J. Phys. Oceanogr., *30,* 2798-2813, 2000

Zhang, R.-H., and S. Levitus, Structure and cycle of decadal variability of upper-ocean temperature in the North Pacific, J. Climate, *10,* 710-727, 1997.

M. Nonaka and S.-P. Xie, International Pacific Research Center/SOEST, University of Hawaii, 2525 Correa Road, Honolulu, Hawaii 96822. (e-mail:nona@soest.hawaii.edu; xie@soest.hawaii.edu)

(Received February 3, 2000; accepted September 1, 2000.)